Physics of Fluids

Roughness-induced critical phenomenon analogy for turbulent friction factor explained by a co-spectral budget model

Cite as: Phys. Fluids **33**, 105127 (2021); https://doi.org/10.1063/5.0069705
Submitted: 01 September 2021 • Accepted: 30 September 2021 • Published Online: 28 October 2021

Shuolin Li and Gabriel Katul

View Online Export Citation CrossMark

ARTICLES YOU MAY BE INTERESTED IN

The law of the wall: A new perspective
Physics of Fluids **32**, 121401 (2020); https://doi.org/10.1063/5.0036387

The effect of entrance flow development on vortex formation and wall shear stress in a curved artery model
Physics of Fluids **33**, 101908 (2021); https://doi.org/10.1063/5.0062565

"Breakdown" of stratified electrical explosion products: Plasma development and its mechanical effect
Physics of Fluids **33**, 107119 (2021); https://doi.org/10.1063/5.0070714

AIP Publishing Author Services
English Language Editing
High-quality assistance from subject specialists
LEARN MORE

AIP Publishing

© 2021 Author(s).

Physics of Fluids ARTICLE scitation.org/journal/phf

Roughness-induced critical phenomenon analogy for turbulent friction factor explained by a co-spectral budget model

Cite as: Phys. Fluids **33**, 105127 (2021); doi: 10.1063/5.0069705
Submitted: 1 September 2021 · Accepted: 30 September 2021 ·
Published Online: 28 October 2021

View Online Export Citation CrossMark

Shuolin Li[a] and Gabriel Katul[b]

AFFILIATIONS

Department of Civil and Environmental Engineering and Nicholas School of the Environment, Duke University, Durham, North Carolina 27708, USA

[a]Author to whom correspondence should be addressed: shuolin.li@duke.edu
[b]gaby@duke.edu

ABSTRACT

Drawing on an analogy to critical phenomena, it was shown that the Nikuradse turbulent friction factor (f_t) measurements in pipes of radius R and wall roughness r can be collapsed onto a one-dimensional curve expressed as a conveyance law $f_t Re^{1/4} = g_o(\chi)$, where Re is the bulk Reynolds number and $\chi = Re^{3/4}(r/R)$. The implicit function $g_o(.)$ was conjectured based on matching two asymptotic limits of f_t. However, the connection between $g_o(.)$ and the phenomenon it proclaims to represent—turbulent eddies—remains lacking. Using models for the wall-normal velocity spectrum and return-to-isotropy for pressure–strain effects to close a co-spectral density budget, a derivation of $g_o(.)$ is offered. The proposed method explicitly derives the solution for the conveyance law and provides a physical interpretation of χ as a dimensionless length scale reflecting the competition between the viscous sublayer thickness and characteristic height of roughness elements. Applications of the proposed method to other published measurements spanning roughness and Reynolds numbers beyond the original Nikuradse range are further discussed.

Published under an exclusive license by AIP Publishing. https://doi.org/10.1063/5.0069705

I. INTRODUCTION

A recent analogy between critical phenomena and turbulent flows was proposed to describe the turbulent friction factor f_t in pipes.[15] The f_t is a dimensionless measure of the total frictional loss along the longitudinal distance (x, along the pipe length) defined as

$$f_t = \frac{(2R)}{\frac{1}{2}\rho_f U_b^2}\frac{\partial P}{\partial x} = \frac{(2R)gS_b}{\frac{1}{2}U_b^2}, \tag{1}$$

and is presumed to vary with the bulk Reynolds number ($Re = 2RU_b/\nu$) and relative roughness of the wall (r/R), where g is the gravitational acceleration, U_b is the bulk or time and cross-area-averaged velocity, r is a measure of the wall roughness commonly related to the statistics of protrusions from the pipe wall, R is the pipe radius, ν is the kinematic viscosity, ρ_f is the fluid density, and S_b is the friction slope that can be related to the driving force—the mean pressure gradient $(\rho_f g)^{-1}\partial P/\partial x$.[6] Using the measured value of f_t, the weighty experiments by Nikuradse[32] on regular roughness elements identified two limiting flow regimes—hydrodynamically smooth and fully rough based on competing mechanisms between r/R and a length scale measuring the thickness of the viscous sublayer ($L_v \sim \eta$ where η is the Kolmogorov micro-scale). In the hydrodynamically smooth case (i.e., $r/L_v \ll 1$), $f_t = A_b Re^{-1/4}$ where $A_b = 0.316$ (labeled as the Blasius scaling) whereas in the fully rough regime ($r/L_v \gg 1$), $f_t = A_s(r/R)^{1/3}$ where $A_s = 0.14$ (labeled as the Strickler scaling). Exploiting an analogy developed to infer the thermodynamic properties of ferromagnets near critical temperatures, the Nikuradse's f_t data were shown to collapse (albeit imperfectly) onto a single curve labeled here as NG06.[15] In the derivation of NG06, two limiting regimes occurring for $r/R \to 0$ (analogous to an external magnetic field control) and $Re^{-1} \to 0$ (analogous to inverse temperature near its critical state), respectively, have been exploited. The NG06 f_t was shown to be mathematically described by[15]

$$f_t = Re^{-1/4} g_o(\chi), \text{ with } g_o(\chi) = \begin{cases} \text{const.}, & \chi \to 0, \\ \chi^{1/3}, & \chi \to \infty, \end{cases} \tag{2}$$

Published under an exclusive license by AIP Publishing

where $\chi = Re^{3/4}(r/R)$ and $g_o(.)$ is an implicit function satisfying two asymptotic properties: when $\chi \to 0$, Eq. (2) yields $f_t \sim Re^{-1/4}$ (the Blasius scaling) whereas at sufficiently large Re, $g_o(\chi)$ becomes $Re^{1/4}(r/R)^{1/3}$ resulting in $f_t \sim (r/R)^{1/3}$ (the Strickler scaling). The outcome of Eq. (2) is a monotonic curve along which all the Nikuradse data collapse as shown in Fig. 1.

The collapse of all Nikuradse data when representing $f_t Re^{1/4}$ as a function of χ may indicate the existence of a critical phenomenon in the turbulent friction factor.[15] The NG06 stimulated other theories and a combination of variables derived from hydrodynamic stability analysis for laminar flow.[26,40] Other approaches for deriving f_t and refinements to NG06 have exploited the so-called spectral link in turbulent flows[1,5,12,13,16,17,31] summarized by

$$f_t \propto \sqrt{\int_{1/l_o}^{\infty} E_{TKE}(k)dk}, \tag{3}$$

where k is the wavenumber or the inverse eddy size, $l_o = r + L_v$, and $E_{TKE}(k)$ is the spectrum of the turbulent kinetic energy (TKE). This relation was tested using soap film experiments where $E_{TKE}(k)$ was manipulated to scale as $k^{-5/3}$ (for 3D turbulence) or k^{-3} (for 2D turbulence) as discussed elsewhere.[17,25,41] Another corollary improvement to NG06 rooted in Eq. (3) was the intermittency corrections to phenomenological models for $E_{TKE}(k)$.[31] When such intermittency corrections are accounted for in $E_{TKE}(k)$, a revised NG06 that better describes the otherwise imperfect fit was reported. The collapse of the Nikuradse data onto a single (albeit in a restricted range of $r/R - Re$) curve is appealing because it offers a diagnostic description of the so-called transitional regime between smooth and fully rough cases[12] or other similarity variants on it.[26] That transitional flow regimes in f_t exhibiting rich scaling laws are now opening up new vistas to other analogies in physics and statistical mechanics[16] though no contact with Navier–Stokes turbulence or approximation to it has been offered to date.

This work explains $g_o(\chi)$ and derives its generalization for steady and axially uniform turbulent pipe flows using standard turbulence arguments. The theoretical tactic employs a co-spectral budget (CSB) model that makes contact with an approximated Navier–Stokes equation for the near-wall turbulent stress in spectral space.[3,9,21,22] The outcome is an analytical formulation linking an externally specified wall-normal energy spectrum to the turbulent stress (via the CSB model), and upon scale-wise integration yields an expression for f_t analogous in form to Eq. (3). This expression includes a bridge between local variables formulated on a plane positioned at a wall distance z_* that scales with l_o and bulk flow variables reflecting the overall geometry and flow rate in the pipe.[3,9] The proposed model is shown to collapse the expanded f_t data onto a single curve whose shape is explicitly derived from the CSB model with all similarity constants linked to standard constants in turbulence theories. Other mechanisms not explicitly treated such as intermittency corrections[31] (or other similarity variants[26]) to the wall-normal velocity spectrum, non-local spectral transfer across scales in energy and stresses, non-linear return-to-isotropy representations for pressure–velocity interactions, or bottle-necks in the energy cascade can all be accommodated in this framework and their effects tracked onto an NG06-type curve but they are not explicitly considered here.

II. THEORY

A. Definitions

The flow is assumed to be stationary and longitudinally homogeneous driven by a constant mean pressure gradient within a pipe of radius R and cross-sectional area A_p. The pipe wall is uniformly covered with regular roughness elements having a protrusion amplitude r similar to the Nikuradse experiments [see Fig. 2(a)]. Defining $z = R - y$ as the normal distance to the pipe boundary, y as the distance from the pipe center, $U^+ = U(z)/u_*$ as the dimensionless mean velocity profile, $u_* = \sqrt{\tau_o/\rho_f}$ as the friction velocity, τ_o as the wall stress, ρ_f as the fluid density, the bulk (i.e., time and cross-sectional area-averaged) velocity can be determined from

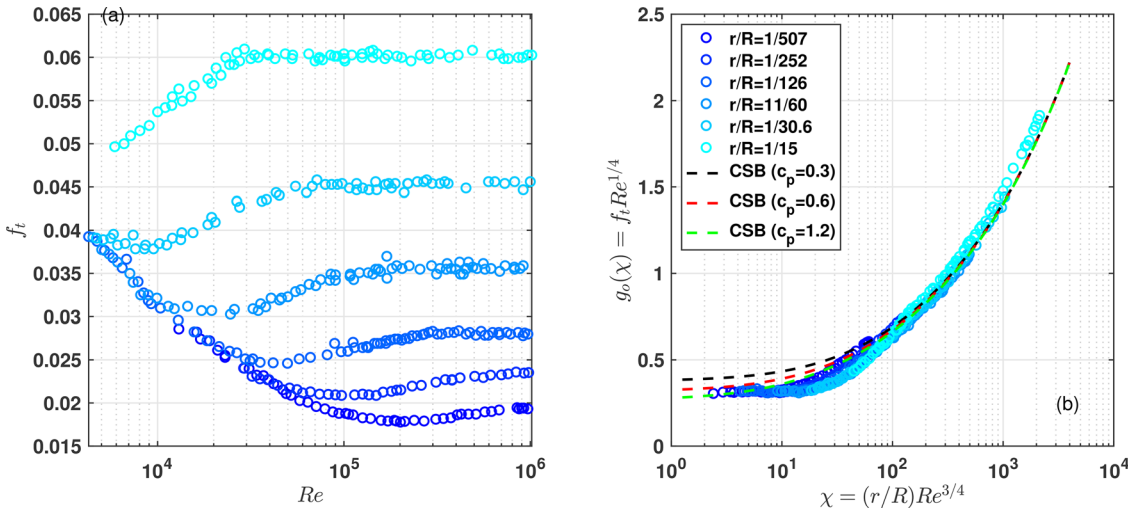

FIG. 1. The original Nikuradse diagram and its NG06 representation with $f_t Re^{1/4}$ expressed as an unknown function of χ. The coefficient $c_p = 0.61$ can be determined when combining Blasius and Strickler scaling relations.[12]

Published under an exclusive license by AIP Publishing

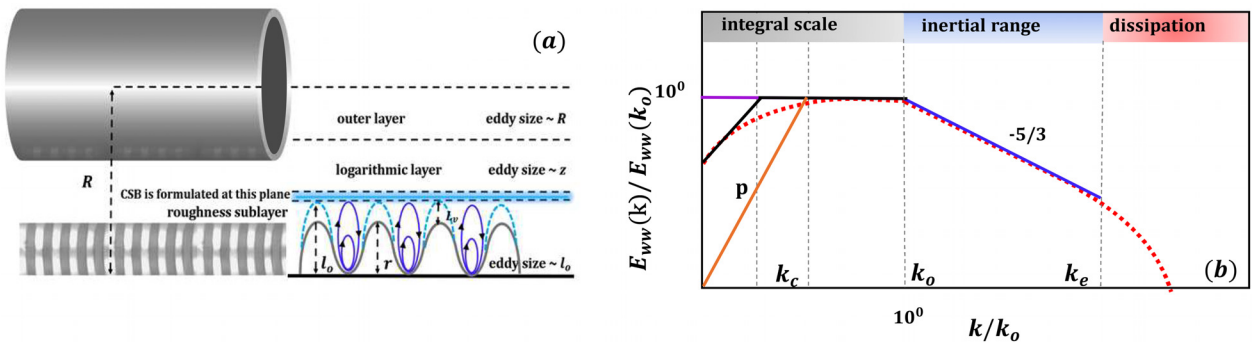

FIG. 2. (a) The formulation of the CSB model at $z_*/l_o > 1$ but below the log-region. (b) Schematic of the wall-normal velocity spectrum $E_{ww}(k)$ of a turbulent rough pipe as a function of wavenumber k. The dashed red line represents commonly observed $E_{ww}(k)$ that can be partitioned into three subranges: an energetic range (integral scale), inertial range, and viscous dissipation range. The solid lines show different models for this spectrum. A plausibility check on the assumed $E_{ww}(k)$ shape can be made using an integral constraint shown in Eq. (15).

$$U_b = \frac{1}{A_p}\int_0^R U(y)dA_s, \tag{4}$$

where $dA_s = 2\pi y dy$. For this setup, the mean longitudinal momentum balance reduces to a balance between the mean pressure gradient and the stress gradient given by

$$\frac{\partial P}{\partial x} = \frac{1}{y}\frac{\partial(y\tau)}{\partial y}, \tag{5}$$

where $\tau(y)$ is the total shear stress at radial distance y from the pipe center. Integrating with respect to y yields

$$\tau(y) = \left(\frac{\partial P}{\partial x}\right)\frac{y}{2} + C_1, \tag{6}$$

where C_1 is determined so that at $y = 0$ (i.e., center of the pipe), $\tau(0) = 0$ due to symmetry, thereby resulting in

$$\tau(y) = \left(\frac{\partial P}{\partial x}\right)\frac{y}{2}. \tag{7}$$

Defining

$$u_*^2 = \frac{\tau_o}{\rho_f} = \frac{1}{\rho_f}\frac{R}{2}\left(\frac{\partial P}{\partial x}\right) = \frac{R}{2}gS_b = \frac{1}{8}f_t U_b^2, \tag{8}$$

and decomposing $\tau(y)$ into a turbulent τ_t and a viscous τ_m contribution leads to the variation in total stress with distance from the wall as

$$\tau(z) = \tau_t + \tau_m = \tau_o\left(1 - \frac{z}{R}\right), \tag{9}$$

where $\tau_m = \rho_f \nu \Gamma(z)$ and $\Gamma(z) = dU/dz$.

B. The co-spectral budget model

The CSB model is now formulated at a wall-normal distance $z = z_*$ below the region where the onset of a logarithmic mean velocity profile for $U^+ = U(z)/u_*$ is expected (Fig. 2). Hence, the effective eddy size l_o impacting momentum exchange at z_* need not scale with z[3,21] but with r or L_v $(= 5\eta/2)$ depending on whether the flow is rough or smooth. To accommodate rough and smooth pipe flow conditions, we define $l_o = r + L_v$ as before,[9,13] where $\eta = (\nu^3/\epsilon)^{1/4}$, and ϵ is a local turbulent kinetic energy dissipation rate evaluated at z_*. A justification for summing r and L_v is that resistances to momentum exchanges between a moving fluid and a stationary wall in the combined layer are additive, and resistances scale linearly with layer thicknesses. The following constraints on the choice of z_* are now enforced: $z_*/l_o \geq 1$ and $\tau_t(z_*)/\tau_o \approx 1$, where $\tau_t(z_*)$ is the turbulent stress at z_* labeled hereafter as τ_* for notational convenience. Selecting z_* to be sufficiently distant from the boundary also minimizes wall-blocking effects impacting U^+ in the buffer region.[29] For a rough pipe, the z_* is still expected to be in the roughness sublayer (RSL) whereas in a turbulent smooth pipe, z_* is in the upper region of the buffer layer.[34–37]

The CSB model links τ_* to eddy sizes at z_* using $\tau_*/\rho_f = -\overline{u'w'} = \int_0^\infty F_{uw}(k)dk$, and $F_{uw}(k)$ defines the co-spectrum between u' and w' at k (or inverse eddy-size)—u' and w' are the turbulent longitudinal and wall-normal velocity components, respectively; primed quantities are excursions from the mean state; and and overline implies averaging over coordinates of statistical homogeneity (usually surrogated to time averaging). The terms governing the time evolution of the co-spectral budget at z_* are[21,22]

$$\frac{\partial F_{uw}(k)}{\partial t} = P_{uw}(k) + T_{uw}(k) + [\pi_{uw}(k) - D_{uw}(k)], \tag{10}$$

where $P_{uw}(k) = \Gamma(z)E_{ww}(k)$ is the turbulent stress production term at wavenumber k due to the presence of a mean velocity gradient Γ, $E_{ww}(k)$ is the energy spectrum of the wall-normal velocity component, $T_{uw}(k)$ is a scale-wise transfer of momentum and satisfies $\int_0^\infty T_{uw}(k)dk = 0$, $\pi_{uw}(k)$ is a pressure–velocity de-correlation term commonly modeled using return-to-isotropy principles, and $D_{uw}(k) = 2\nu k^2 F_{uw}(k)$ is a viscous dissipation term also responsible for de-correlating u' from w'. Stationarity is assumed throughout and closure models for $\pi_{uw}(k)$ and $T_{uw}(k)$ are needed. For maximum simplicity and to ensure a recovery of $F_{uw}(k) \propto k^{-7/3}$ in the so-called inertial subrange (ISR), $T_{uw}(k) = 0$ is assumed (and justified later on). Adopting a linear Rotta scheme revised for isotropization of the production at any k, $\pi_{uw}(k)$ is closed by[3,9,21,22,29]

$$\pi_{uw}(k) = -C_R\frac{1}{t_r(k)}F_{uw}(k) - C_I P_{uw}(k), \tag{11}$$

Published under an exclusive license by AIP Publishing

where $C_R \approx 1.8$ and $C_I = 3/5$[35] are the Rotta and isotropization of production constants, and $t_r(k) = [k^3 E_{kol}(k)]^{-1/2}$ is a local wavenumber-dependent relaxation time scale[33,35] based on a Kolmogorov spectrum $E_{kol}(k)$. Other possibilities that include non-local energy transfer can be accommodated using $t_r(k)$. For example, a non-local closure for the energy flux is the Heisenberg model[18] that can be re-cast as $t_r(k)^{-1} = \sqrt{\int_0^k p^2 E_{kol}(p)dp}$.[23] There are issues with the Heisenberg model related to the directional energy transfer and equipartition of energy that have already been identified and discussed.[7] For this reason, the focus here is maintained on the simpler $t_r(k) = [k^3 E_{kol}(k)]^{-1/2}$. The $t_r(k)$ becomes unbounded as $k \to 0$, necessitating additional constraints at large scales. One possible constraint is to set $t_r(k) = t_r(k_c)$ when $k/k_c < 1$ where $k_c = 1/R$ is the smallest inverse length scale over which $E_{ww}(k)$ energy transfer occurs downscale. The two destruction terms in the CSB model, the Rotta component of $\pi_{uw}(k)$ and viscous destruction $D_{uw}(k)$, are compared at small scales (or large k) using

$$\Phi(k) = \frac{2\nu k^2 F_{uw}(k)}{C_R F_{uw}(k)/t_r(k)} = \frac{2}{C_R}(k\eta)^{4/3}, \tag{12}$$

where the role of $P_{uw}(k)$ has been ignored at large k for simplicity. When $k\eta \ll 1$, the viscous dissipation is negligible ($\Phi(k) \approx 0$) compared with the Rotta term. However, as $k\eta > 1$, the viscous term dominates and $\Phi^{-1}(k) \approx 0$. Adopting the aforementioned closure schemes, the co-spectrum at k is derived as

$$F_{uw}(k) = \frac{1 - C_I}{C_R}\Gamma(z_*)\frac{E_{ww}(k)t_r(k)}{\Phi(k) + 1}. \tag{13}$$

The co-spectrum must be integrated across all k to yield τ_* needed in the determination of f_t. To evaluate $F_{uw}(k)$, the shape of $E_{ww}(k)$ is required and discussed in Fig. 2.

The $E_{ww}(k)$ in the ISR is given by the Kolmogorov spectrum $E_{kol}(k) = C_o[\epsilon(z_*)]^{2/3}k^{-5/3}$, where $C_o = (24/55)C_o'$ is the Kolmogorov constant for the wall-normal velocity component[35] related to the Kolmogorov constant for the turbulent kinetic energy spectrum ($C_o' = 1.5$). Deviations from E_{kol} at other scales are specified as follows: (i) an exponential cutoff, $f_\eta = \exp[-\beta(\frac{1}{2}C_R\Phi)^{3/4}] \approx 1$ when $k \ll k_e$, where $\beta = 2.1$, to resolve the viscous dissipation range;[14,35] (ii) two piece-wise functions for the energetic range.[3] The $E_{ww}(k)$ is

$$E_{ww}(k) = \begin{cases} E_{kol}(k_o)k_c^{-p}k^p & \text{if } 0 \le k \le k_c \\ E_{kol}(k_o) & \text{if } k_c \le k \le k_o \\ E_{kol}(k)f_\eta & \text{otherwise,} \end{cases} \tag{14}$$

where $k_c = 1/R$, $k_o = 1/l_o$, and $k_e = 1/\eta$ are three characteristic wavenumbers that mark the key transitions in $E_{ww}(k)$ as related to pipe radius, characteristic eddy scale in the RSL, and the viscous length scale,[3,9,22,27,35] and several theories constrain p to lie between 2 (Saffman spectrum) and 4 (Batchelor spectrum). The p remains uncertain though various turbulence theories suggest a numerical value of $p = 2$ (Saffman spectrum), $p = 8/3$ (von Kármán spectrum), or $p = 4$ (Batchelor spectrum) reviewed elsewhere.[35] All theories agree that $p > 1$ to ensure that as $k \to 0$, both $E_{ww}(k) \to 0$ and $(dE_{ww}(k)/dk) \sim k^{p-1} \to 0$. Not withstanding this uncertainty in p, its precise numerical value does not alter the scale-wise integrated outcome. A plausibility check on the assumed shape of $E_{ww}(k)$ is conducted using the integral constraint $\sigma_w^2 = \int_0^\infty E_{ww}(k)dk$, yielding

$$\sigma_w^2 \approx \left[1.63 - \frac{0.65p}{p+1}\left(\frac{l_o}{R}\right) - 0.69\left(\frac{\eta}{l_o}\right)^{2/3}\right]u_*^2, \tag{15}$$

where a balance between the production and dissipation of TKE yields $\epsilon(z_*) \approx u_*^2\Gamma(z_*)$ and $\Gamma(z_*) = u_*/l_o$. Equation (15) predicts a maximum $\sigma_w/u_* = \sqrt{1.63} = 1.28$ sufficiently close to the reported $1.1 - 1.25$ range in near-neutral atmospheric flows, open channels, and pipes.[9,20,34,36,37]

Equation (13) can be further analyzed for the much-studied ISR and is shown to be consistent in both scaling law and similarity coefficients with accepted theories and experiments.[35,38] For example, in the ISR, $\Phi(k) \ll 1$, and the co-spectrum reduces to

$$F_{uw}(k) = \sqrt{C_o}\frac{(1 - C_I)}{C_R}\Gamma(z_*)[\epsilon(z_*)]^{1/3}k^{-7/3}, \tag{16}$$

consistent with well-accepted co-spectral theories predicting $k^{-7/3}$ scaling.[28,35] The emerging constants $\sqrt{C_o}(1 - C_I)/C_R = 0.18$ are also close to the accepted similarity constant reported in laboratory and field experiments as well as direct numerical simulations ($= 0.15$) discussed elsewhere.[4,22,38,42] These findings indirectly support setting $T_{uw}(k) = 0$ for all k as a first-order approximation in two ways: (i) its expected zero value in the ISR is needed to recover the $k^{-7/3}$ scaling and (ii) $T_{uw}(k)$ must satisfy the integral constraint $\int_0^\infty T_{uw}(k)dk = 0$ by definition. In the case of $E_{kol}(k)$, the transfer of energy across scales shapes the energy cascade and is thus necessary for obtaining the $k^{-5/3}$ scaling in the ISR. The inclusion of the transfer term in the energy cascade [indirectly specified by $E_{ww}(k)$] but not in the CSB may appear paradoxical. This is not so as the role and significance of the transfer terms are quite different when analyzing scale-wise energy and scale-wise stress budgets.[4] Last, when $\Gamma(z) = 0$, $F_{uw}(k) = 0$ at all k. Hence, a finite $\Gamma(z_*)$ is necessary to maintain a finite co-spectrum at all k and $f_t > 0$.

Returning to the determination of f_t, upon inserting Eq. (14) into (13) yields the near-bed shear stress in terms of $f_t(= 8\tau_*/\rho_f U_b^2)$ as

$$\frac{f_t U_b^2}{8} = \frac{\xi(z_*)}{A_\pi}\left[\int_0^{k_c} k_c^{-p-2/3}k_o^{-5/3}k^p dk + \int_{k_c}^{k_o} k_o^{-5/3}k^{-2/3}dk + \int_{k_o}^{k_e} k^{-7/3}dk + B_\pi\int_{k_e}^{+\infty} k_e^{4/3}k^{-11/3}\exp(-\beta k\eta)dk\right], \tag{17}$$

where $A_\pi = C_R/[\sqrt{C_o}(1 - C_I)] \approx 5.58$, $B_\pi = (5^{4/3}/2)C_R\sqrt{C_o} \approx 6.20$, and $\xi(z_*) = \Gamma(z_*)[\epsilon(z_*)]^{1/3}$. The four integrand functions are contributions to the turbulent stress arising from the two energetic, inertial, and dissipation ranges, respectively.

III. RESULTS

A. Linking local and bulk variables

The terms $\Gamma(z_*)$ and $\epsilon(z_*)$ needed in $\xi(z_*)$ are defined at z_* and must be linked to bulk variables to complete the CSB model for f_t. These are commonly estimated as[3,9]

$$\Gamma(z_*) = \frac{u_*}{l_o} = c_t\frac{U_b - 0}{l_o}, \quad \epsilon(z_*) = \frac{u_*^3}{l_o} = c_p^3\frac{U_b^3}{R}, \tag{18}$$

Published under an exclusive license by AIP Publishing

where $c_t(z_*)$ and $c_p(z_*)$ are unknown positive coefficients that link local to bulk variables given by $c_t = u_*/U_b$ and $c_p = (u_*/U_b)(R/l_o)^{1/3} = c_t(R/l_o)^{1/3}$. A bulk dissipation proportional to U_b^3/R is compatible with upper limits set by prior variational analysis.[10] Clearly, c_t and c_p cannot be individually constant and must vary with f_t.[3,9] The interest here is not in their individual variations but in their product. Increasing l_o increases c_p (more dissipation for the same U_b or flow rate) but decreases c_t because U_b overestimates $U(z_*)$, thus making their product less sensitive to l_o as shown elsewhere.[3,9]

For guessing a c_tc_p, several possibilities exist including the use of complete and incomplete similarity or covariate analysis.[2] Another naive possibility is to assume c_tc_p varies with the primary variable R/l_o and proceed to select a minimal c_tc_p at a given R/l_o (e.g., analogous to drag deduction). By definition, $c_tc_p \sim (u_*/U_b)^2(R/l_o)^{1/3}$. With $s = R/l_o$, assuming $G_f(s) = (u_*/U_b)^2$ and minimizing c_tc_p at a given s leads to

$$\frac{d}{ds}(c_tc_p) = \left[\frac{G_f(s)}{3s^{2/3}} + s^{1/3}\frac{d}{ds}G_f(s)\right] = 0. \tag{19}$$

The solution of Eq. (19) is $G_f(s) = b_o s^{-1/3}$, where b_o is a constant independent of $s = R/l_o$. This argument is congruent with complete similarity theory in the limit of very large R/l_o but cannot be correct for all R/l_o. Accepting momentarily a constant c_tc_p at its minimal value, f_t can be linked to r/R and Re at any finite R/l_o using

$$f_t = \frac{30(c_tc_p)}{A_\pi}\left[-Y(p)\left(\frac{k_c}{k_o}\right)^{2/3} + \left(\frac{k_c}{k_o}\right)^{1/3} - C_\pi\left(\frac{k_c}{k_e}\right)^{1/3}\frac{k_o}{k_e}\right], \tag{20}$$

where

$$Y(p) = \frac{12p+8}{15(p+1)}, \quad C_\pi = \frac{1}{5} - \frac{4\sqrt[3]{5}}{1875}\beta^{\frac{8}{3}}\Gamma_{o,*}\left(-\frac{8}{3},\frac{\beta}{5}\right),$$

$\Gamma_{o,*}(.)$ is the Gamma function and $C_\pi \approx 0.146$. For $p = 2-4$, $Y(p) \approx 0.72 - 0.75$ and variations in p are hereafter ignored. The two extreme cases, Strickler and Blasius scaling are now evaluated. In a rough pipe where $r/L_v \gg 1$, $DS(k)$ can be ignored and $k_e = k_o(r/\eta) \to \infty$ allowing the ISR to extend to $k_e \to \infty$. In the limit of $r/R \ll 1$, the leading order term in Eq. (20) is

$$f_t \approx \frac{30}{A_\pi}c_pc_t\left(\frac{r}{R}\right)^{1/3}. \tag{21}$$

Hence, the Stickler scaling requires (i) a constant c_pc_t $(= A_sA_\pi/30 \approx 0.026$ to recover the Nikuradse data), (ii) $r/L_v \gg 1$, and (iii) $r/R \ll 1$. Likewise, when $r/L_v \ll 1$ so that $l_o \approx L_v$, the inertial subrange commences at k_e and rapidly terminates into a dissipation range since $k_r/k_e \ll 1$. The viscous cutoff effects become important when $k > k_e$ revising Eq. (20) to

$$f_t \approx \frac{30D_\pi}{A_\pi}c_tc_p\left(\frac{\eta}{R}\right)^{1/3} = \frac{30D_\pi}{2^{-1/4}A_\pi}c_tc_p^{3/4}Re^{-1/4}, \tag{22}$$

where $D_\pi = \sqrt[3]{5} - C_\pi/5 \approx 1.68$, $(R/\eta)^{1/3} = (c_pRe/2)^{1/4}$. The Blasius scaling requires $c_tc_p^{3/4}$ $[= 2^{-1/4}A_bA_\pi/(30D_\pi) \approx 0.0294$ for the Nikuradse data] not to vary with Re (or equivalently c_tc_p not to vary with R/l_o when $l_o = L_v$ as before). Equation (20) allows to separate the effects of turbulent exchanges of momentum at z_* from relations between local (at z_*) and bulk variables (encoded in c_tc_p) when evaluating f_t or NG06. Prior knowledge of either c_tc_p or f_t is required to overcome a circular argument discussed elsewhere.[3] However, the merit of using c_tc_p is that the contribution of momentum exchange to the friction factor can be now separated explaining the origin of relative length scale R/l_o in existing f_t formulations.

B. Solution of the implicit function in NG06

The study objective, which is to derive the $g_o(\chi)$ in NG06 for the Nikuradse data $(r/R \ll 1)$ and regular roughness, can now be addressed. The $g_o(\chi)$ can be made explicit when rearranging Eq. (20) to yield

$$g_o(\chi) = (c_tc_p^{3/4})\frac{30}{2^{-1/4}A_\pi}\left\{\left[\left(\frac{c_p}{2}\right)^{3/4}\chi + 5\right]^{1/3} - C_\pi\left[\left(\frac{c_p}{2}\right)^{3/4}\chi + 5\right]^{-1}\right\}, \tag{23}$$

where $\chi = Re^{3/4}(r/R)$ derived from $\chi = (2/c_p)^{3/4}(r/\eta)$. Now, Eq. (23) explains why the Nikuradse data imperfectly collapse along a unique curve when plotting $f_tRe^{1/4}$ vs $Re^{3/4}(r/R)$ under the restrictive assumption of constant c_tc_p. Thus, the main novelty here is to show that the $g_o(\chi)$ in NG06 can be linked to an approximated Navier–Stokes equation (i.e., the CSB model) provided c_tc_p is constant at minimal value, which is the sought result. The solution of Eq. (23) is also presented in Fig. 1 where $c_p = 2(D_\pi A_s/A_b)^4 \approx 0.6$ and can be directly derived when combining the Strickler and Blasius scaling laws. Moreover, a sensitivity analysis was conducted by setting $c_p = 0.3, 1.2$ to find the best fit between Eq. (23) and the Nikuradse dataset. Figure 1 shows that setting c_p as constant (accepting Blasius and Strickler scaling laws simultaneously) can indeed replicate the NG06 result to a leading order, but further investigations are needed when $\chi < 20$.

IV. DISCUSSION

A. Extension to micro-scale and large-scale roughness

Moving beyond the widely used Nikuradse data range for $r/R < 0.1$ and for regular roughness elements, the following discussion is presented to assess the plausibility of extending the implicit function $g_o(\chi)$ to two extreme cases as shown in Fig. 3: (i) a hydrodynamically smooth regime or the micro-scale roughness $r/R \in [10^{-6}, 10^{-5}]$ from Hi-Reff[11] superpipe experiments (the Oregon and Princeton[30,39] are assumed smooth though no r/R measurements were reported) and (ii) a large-scale roughness regime $r/R \in [0.1, 0.2]$ from pipes roughened with single layers of sand.[19] The reported friction factor data[19] (runs $R4$ and $R5$) in their original Table I were employed. These two runs can still be approximated as regular roughness with r/R not too large so that the prior conditions imposed on z_* for the use of the CSB can still be enforced.

B. Estimation of c_tc_p

To extend the proposed model and without invoking further *ad hoc* assumptions on the local flow structure, a "naïve" but direct approach is to revise the constant c_t c_p assumption that seems only applicable to the Nikuradse range.[9,12] When inferring U_b, the log-law is assumed to populate U^+ over extensive portions of the pipe area at intermediate to high Re. The log-law overestimates U^+ in the buffer region (for smooth pipes) or the roughness sublayer (in rough pipes)

Published under an exclusive license by AIP Publishing

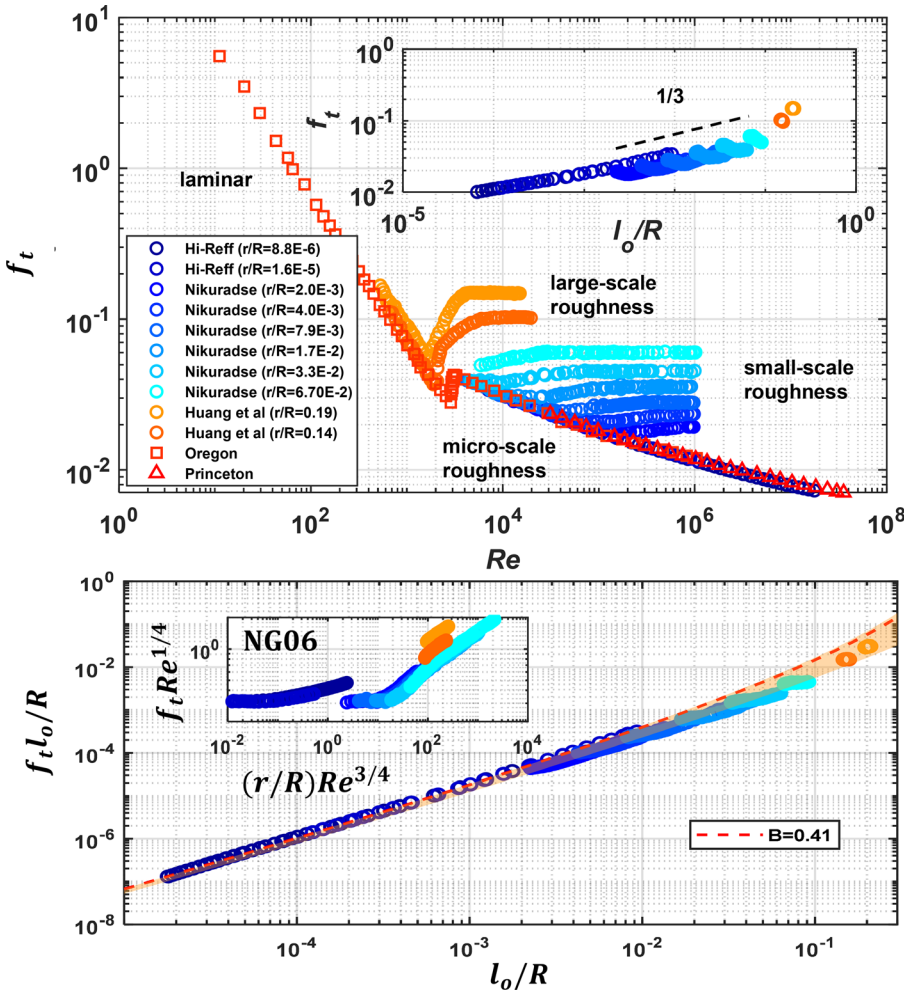

FIG. 3. Representation of f_t across regular roughness elements. The top panel shows the expanded Nikuradse diagram using wider experimental conditions, including the large-scale roughness,[19] intermediate/small-scale roughness,[32] and smooth wall.[11,30,39] The inset is a representation of all f_t with l_o/R as a general scale using the turbulence data (excluding non-turbulent regimes). The bottom panel shows the data collapse of $f_t(l_o/R)$ vs l_o/R where the orange band features CSB prediction with $B_o \in [0.04, 4]$. The inset is the NG06 curve for the same data.

but underestimates U^+ in the wake-region.[21] Thus, its area-integrated form from l_o to R may be less sensitive to such deviations and provides a leading order guess as to whether $c_t c_p$ is constant or variable. With this idealized U^+ representation, it follows that $c_t^{-1} \approx U_b/u_* = (1/\kappa)\ln(R/l_o) + B_o$, where B_o is an integration constant of order unity and κ is the von Kármán constant.[35] For this c_t and $c_p = c_t(R/l_o)^{1/3}$, their product can now be estimated as

$$c_t c_p \approx \left(\frac{R}{l_o}\right)^{\frac{1}{3}} \left[\frac{1}{\kappa}\ln\left(\frac{R}{l_o}\right) + B_o\right]^{-2}. \tag{24}$$

Increasing R/l_o increases both the numerator and denominator thereby making their ratio less sensitive to R/l_o as expected. However, a near constant $c_t c_p$ emerges when noting that for large but finite R/l_o, $\ln(R/l_o) \approx A_n(R/l_o)^{n_o}$ with $n_o = 1/6$ for the range covered by R/l_o in many experiments.[24] To elaborate, the limiting case for large R/l_o is considered and this case leads to

$$n_o \approx \lim_{R/l_o \to \infty} \frac{\log[\log(R/l_o)]}{\log(A_n) + \log(R/l_o)} \approx \frac{1}{\log(R/l_o)}, \tag{25}$$

when applying l'Hôpital's rule. The $n_o = 1/\log(R/l_o)$ appears independent of A_n but weakly depends on R/l_o as shown from a similar argument using asymptotic covariance analysis.[2] In general, $n_o \to 1/\log(R/l_o)$ for very large R/l_o and cannot be a constant. To explore the plausibility of setting $c_t c_p$ a constant beyond the Nikuradse experiments, other predictions from the virtual Nikuradse[43] equation (VN), the Moody diagram summarized by the approximate von Kármán equation,[8] and the aforementioned micro-scale and large-scale roughness data are employed and discussed in Fig. 4.

Figure 4 shows that $c_t c_p$ does not vary appreciably with r/R for small-scale roughness ($r/R < 0.1$) consistent with the range of applicability.[3,9] However, as r/R increases to 0.2, $c_t c_p$ increases leading to a breakdown in the Strickler scaling. This breakdown originates from estimates of $\xi(z_*)$ when using bulk variables and not in the particulars of momentum exchange by turbulent eddies at z_* represented by the CSB model. Likewise, for the Blasius scaling the $c_t c_p^{3/4}$ (or $c_t c_p$ independent of R/L_v) remains flat for a restricted range of $Re \in [10^4, 10^5]$ but increases significantly with increasing Re.

With modeled $c_t c_p$ provided in Eq. (24), a representation of extended Nikuradese diagram with additional micro-scale and

Published under an exclusive license by AIP Publishing

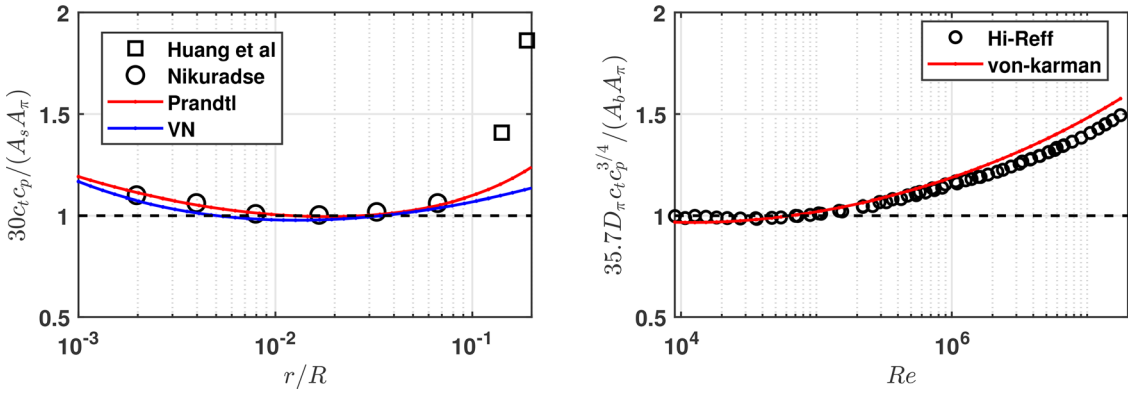

FIG. 4. Exploring the similarity coefficient of Strickler and Blasius scaling relations. The datasets are normalized by A_s and A_b, the similarity coefficients for the Strickler and Blasius formulas, respectively, where the black dashed line is unity. Other than the experimental data (Nikuradse and Huang *et al.*), the red lines represent the predictions from Prandtl and von Kármán equations (or the Colebrook–White formula when added), and the blue line features predictions from the virtual Nikuradse (VN) curve.

large-scale roughness data is also shown in Fig. 3. Figure 3 shows that all these f_t data reasonably collapse along a one-dimensional curve (predicted from CSB) when plotted against l_o/R. This finding indicates that l_o/R is a characteristic length scale that describes f_t in all regimes as alluded to in earlier studies.[3,9] Similar to the data collapse strategy that NG06 employed, an apparent curve can also be derived when plotting $f_t \cdot (l_o/R)$ vs l_o/R, where $f_t \cdot (l_o/R)$ can be understood physically as a "roughness friction factor" noting that $f_t(l_o/R) = 2gl_oS_b/U_b^2$. The improved data collapse from the $f_t \cdot (l_o/R)$ representation is partly connected to self-correlation because the abscissa and ordinate now share the same variable (l_o/R) that span several orders of magnitude. Likewise, the NG06 representation also suffers from similar self-correlation through Re, which varies over several orders of magnitude as well. This finding confirms the applicability of the proposed CSB model at the two extremes of (l_o/R) albeit models for $c_t c_p$ are required as deviations from a constant product value are expected. These deviations are connected to how the bulk variables relate to local mean velocity gradient and TKE dissipation rate at z_* instead of how eddies transport momentum to pipe walls at z_*.

V. CONCLUSION

An explicit solution for the NG06 conveyance equation for friction factor, originally conjectured from analogies to the critical phenomenon, was derived from a CSB model. The CSB model employs standard turbulent theories and a commonly accepted wall-normal velocity spectrum. The model closes the pressure–velocity de-correlation term using a linear Rotta scheme based on linear return-to-isotropy with adjustments due to isotropization of the production term. Moving beyond and above the CSB model, the extension of CSB prediction is also discussed in terms of micro-scale roughness and large-scale roughness experiments that were not covered by the original Nikuradse range. The analysis shows that all the turbulent friction factor data collected so far can be approximately collapsed onto a single curve. However, the work here shows that much of the uncertainty originates from how local to bulk variables are related instead of the mechanics of momentum exchange with the pipe walls.

ACKNOWLEDGMENTS

Support from the U.S. National Science Foundation (Nos. NSF-AGS-1644382, NSF-AGS-2028633, and NSF-IOS-1754893) is acknowledged.

AUTHOR DECLARATIONS

Conflict of Interest

The authors have no conflicts to disclose.

DATA AVAILABILITY

All the data used in this work are collected from studies published in Refs. 11, 19, 30, 32, and 39.

REFERENCES

[1]H. R. Anbarlooei, D. O. A. Cruz, and F. Ramos, "New power-law scaling for friction factor of extreme Reynolds number pipe flows," Phys. Fluids **32**(9), 095121 (2020).
[2]G. I. Barenblatt and N. Goldenfeld, "Does fully developed turbulence exist? Reynolds number independence versus asymptotic covariance," Phys. Fluids **7**(12), 3078–3082 (1995).
[3]S. Bonetti, G. Manoli, C. Manes, A. Porporato, and G. G. Katul, "Manning's formula and Strickler's scaling explained by a co-spectral budget model," J. Fluid Mech. **812**, 1189–1212 (2017).
[4]W. J. T. Bos, H. Touil, L. Shao, and J.-P. Bertoglio, "On the behavior of the velocity-scalar cross correlation spectrum in the inertial range," Phys. Fluids **16**(10), 3818–3823 (2004).
[5]E. Calzetta, "Friction factor for turbulent flow in rough pipes from Heisenberg's closure hypothesis," Phys. Rev. E **79**(5), 056311 (2009).
[6]M. M. Clark, *Transport Modeling for Environmental Engineers and Scientists* (John Wiley & Sons, 2011).
[7]T. T. Clark, R. Rubinstein, and J. Weinstock, "Reassessment of the classical turbulence closures: The Leith diffusion model," J. Turbul. **10**, N35 (2009).
[8]C. F. Colebrook, T. Blench, H. Chatley, E. H. Essex, J. R. Finniecome, G. Lacey, J. Williamson, and G. G. Macdonald, "Correspondence: Turbulent flow in pipes with particular reference to the transition region between the smooth and rough pipe laws (includes plates)," J. Inst. Civil Eng. **12**(8), 393–422 (1939).
[9]F. Coscarella, R. Gaudio, G. G. Katul, and C. Manes, "Relation between the spectral properties of wall turbulence and the scaling of the Darcy-Weisbach friction factor," Phys. Rev. Fluids **6**(5), 054601 (2021).
[10]C. R. Doering and P. Constantin, "Variational bounds on energy dissipation in incompressible flows: Shear flow," Phys. Rev. E **49**(5), 4087 (1994).

Published under an exclusive license by AIP Publishing

[11]N. Furuichi, Y. Terao, Y. Wada, and Y. Tsuji, "Friction factor and mean velocity profile for pipe flow at high Reynolds numbers," Phys. Fluids **27**(9), 095108 (2015).
[12]G. Gioia and F. A. Bombardelli, "Scaling and similarity in rough channel flows," Phys. Rev. Lett. **88**(1), 014501 (2001).
[13]G. Gioia and P. Chakraborty, "Turbulent friction in rough pipes and the energy spectrum of the phenomenological theory," Phys. Rev. Lett. **96**(4), 044502 (2006).
[14]G. Gioia, N. Guttenberg, N. Goldenfeld, and P. Chakraborty, "Spectral theory of the turbulent mean-velocity profile," Phys. Rev. Lett. **105**(18), 184501 (2010).
[15]N. Goldenfeld, "Roughness-induced critical phenomena in a turbulent flow," Phys. Rev. Lett. **96**(4), 044503 (2006).
[16]N. Goldenfeld and H. Y. Shih, "Turbulence as a problem in non-equilibrium statistical mechanics," J. Stat. Phys. **167**(3–4), 575–594 (2017).
[17]N. Guttenberg and N. Goldenfeld, "Friction factor of two-dimensional rough-boundary turbulent soap film flows," Phys. Rev. E **79**(6), 065306 (2009).
[18]W. Heisenberg, "On the theory of statistical and isotropic turbulence," Proc. R. Soc. London, Ser. A **195**(1042), 402–406 (1948).
[19]K. Huang, J. W. Wan, C. X. Chen, Y. Q. Li, D. F. Mao, and M. Y. Zhang, "Experimental investigation on friction factor in pipes with large roughness," Exp. Therm. Fluid Sci. **50**, 147–153 (2013).
[20]G. G. Katul, P. L. Finkelstein, J. F. Clarke, and T. G. Ellestad, "An investigation of the conditional sampling method used to estimate fluxes of active, reactive, and passive scalars," J. Appl. Meteorol. **35**(10), 1835–1845 (1996).
[21]G. G. Katul and C. Manes, "Cospectral budget of turbulence explains the bulk properties of smooth pipe flow," Phys. Rev. E **90**(6), 063008 (2014).
[22]G. G. Katul, A. Porporato, C. Manes, and C. Meneveau, "Co-spectrum and mean velocity in turbulent boundary layers," Phys. Fluids **25**(9), 091702 (2013).
[23]G. Katul, A. Porporato, and V. Nikora, "Existence of k^{-1} power-law scaling in the equilibrium regions of wall-bounded turbulence explained by Heisenberg's eddy viscosity," Phys. Rev. E **86**(6), 066311 (2012).
[24]G. Katul, P. Wiberg, J. D. Albertson, and G. Hornberger, "A mixing layer theory for flow resistance in shallow streams," Water Resour. Res. **38**(11), 32-1–32-8, https://doi.org/10.1029/2001WR000817 (2002).
[25]H. Kellay, T. Tran, W. Goldburg, N. Goldenfeld, G. Gioia, and P. Chakraborty, "Testing a missing spectral link in turbulence," Phys. Rev. Lett. **109**(25), 254502 (2012).
[26]S. Li and W. Huai, "United formula for the friction factor in the turbulent region of pipe flow," PLoS One **11**(5), e0154408 (2016).
[27]S. Li and G. Katul, "Cospectral budget model describes incipient sediment motion in turbulent flows," Phys. Rev. Fluids **4**(9), 093801 (2019).
[28]J. L. Lumley, "Similarity and the turbulent energy spectrum," Phys. Fluids **10**(4), 855–858 (1967).
[29]K. A. McColl, G. G. Katul, P. Gentine, and D. Entekhabi, "Mean-velocity profile of smooth channel flow explained by a cospectral budget model with wall-blockage," Phys. Fluids **28**(3), 035107 (2016).
[30]B. J. McKeon, C. J. Swanson, M. V. Zagarola, R. J. Donnelly, and A. J. Smits, "Friction factors for smooth pipe flow," J. Fluid Mech. **511**, 41 (2004).
[31]M. Mehrafarin and N. Pourtolami, "Intermittency and rough-pipe turbulence," Phys. Rev. E **77**(5), 055304 (2008).
[32]J. Nikuradse *et al.*, *Laws of Flow in Rough Pipes* (National Advisory Committee for Aeronautics Washington, 1950), Vol. 2.
[33]L. Onsager, "Statistical hydrodynamics," Il Nuovo Cimento **6**(2), 279–287 (1949).
[34]D. Poggi, A. Porporato, and L. Ridolfi, "An experimental contribution to near-wall measurements by means of a special laser Doppler anemometry technique," Exp. Fluids **32**(3), 366–375 (2002).
[35]S. B. Pope, *Turbulent Flows* (Cambridge University Press, Cambridge, 2000).
[36]M. R. Raupach, "Conditional statistics of Reynolds stress in rough-wall and smooth-wall turbulent boundary layers," J. Fluid Mech. **108**, 363–382 (1981).
[37]M. R. Raupach, R. A. Antonia, and S. Rajagopalan, "Rough-wall turbulent boundary layers," Appl. Mech. Rev. **44**(1), 1–25 (1991).
[38]S. G. Saddoughi and S. V. Veeravalli, "Local isotropy in turbulent boundary layers at high Reynolds number," J. Fluid Mech. **268**, 333–372 (1994).
[39]C. J. Swanson, B. Julian, G. G. Ihas, and R. J. Donnelly, "Pipe flow measurements over a wide range of Reynolds numbers using liquid helium and various gases," J. Fluid Mech. **461**, 51 (2002).
[40]J. Tao, "Critical instability and friction scaling of fluid flows through pipes with rough inner surfaces," Phys. Rev. Lett. **103**(26), 264502 (2009).
[41]T. Tran, P. Chakraborty, N. Guttenberg, A. Prescott, H. Kellay, W. Goldburg, N. Goldenfeld, and G. Gioia, "Macroscopic effects of the spectral structure in turbulent flows," Nat. Phys. **6**(6), 438 (2010).
[42]J. C. Wyngaard and O. R. Coté, "Cospectral similarity in the atmospheric surface layer," Q. J. R. Meteorol. Soc. **98**(417), 590–603 (1972).
[43]B. H. Yang and D. D. Joseph, "Virtual Nikuradse," J. Turbul. **10**, N11 (2009).

Published under an exclusive license by AIP Publishing